Code Shift Keying Impulse Modulation for UWB Communications

Serhat Erküçük, *Member, IEEE,* Dong In Kim, *Senior Member, IEEE,* and Kyung Sup Kwak

***Abstract*—In this paper, the system performance of M-ary code shift keying (MCSK) impulse modulation is studied in detail and compared to M-ary pulse position modulation (MPPM) under single- and multi-user scenarios. For that, bounds on the semi-analytic symbol-error rate (SER) expressions are derived and simulation studies are conducted. When *practical* implementations of MCSK and MPPM are considered, it is shown that MCSK can provide about 2 dB performance gain over MPPM as it reduces the effects of multipath delays on the decision variables by randomizing locations of the transmit pulse.**

***Index Terms*—M-ary code shift keying (MCSK), impulse radios (IRs), ultra wideband (UWB) communications, randomized locations of the transmit pulse.**

I. Introduction

ULTRA wideband impulse radio (UWB-IR) technology [1] is an attractive choice to support high-rate data communications and low-rate precise location and ranging. Time-hopping M-ary pulse position modulation (TH-MPPM) has been considered as the main modulation format to meet the demand for higher data rates [2]. In the conventional implementation of MPPM, a single pulse is transmitted in one of the fixed M consecutive pulse positions. In a multipath channel, energy collected from consecutive pulse locations may be interfered by a large portion of multipath-delayed received pulses. This may generate noticeable interference components for the M decision variables, and hence may affect the system performance.

To reduce the effect of interference components, one approach is to randomize the consecutive pulse transmit locations using M orthogonal TH codes. With this approach, (i) the separation between consecutive pulse positions can be increased while the data rate is fixed, and (ii) multiple-access capability can still be maintained with the random selection of user-specific TH codes. We refer to this new modulation format as M-ary code shift keying (MCSK) impulse modulation. We initially proposed MCSK as a combined modulation with binary PPM (BPPM) in [3] in order to increase the data rate of the conventional TH-BPPM. Combined MCSK/BPPM provided improved system performance at higher data rate if the system design parameters were properly selected. In this paper, MCSK impulse modulation is considered by itself, and studied in detail for comparison to TH-MPPM.

MCSK is considered here for both single- and multi-user cases. In the study of single-user case, the effect of multipath-delayed pulses on M decision variables is explicitly provided in terms of channel impulse response coefficients. In the study of multi-user case, an accurate semi-analytic symbol-error rate (SER) expression is derived by considering the *generalized* Gaussian distribution (GGD) presented in [4] for multi-user interference (MUI) modelling. Some approximations to MUI modelling are provided in the Results Section. These approximations increase the computational efficiency of numerical analysis significantly with respect to simulations, while still providing accurate results. For both single- and multi-user cases, it is shown that MCSK can provide about 2 dB performance gain over MPPM as it reduces the effects of multipath delays on the decision variables by randomizing locations of the transmit pulse. This performance gain is mainly a result of separated M decision variables experiencing less interference due to the decaying power delay profile.

Manuscript received March 23, 2007; revised May 25, 2007; accepted July 14, 2007. The associate editor coordinating the review of this letter and approving it for publication was E. Serpedin. This work was supported by the MKE (Ministry of Knowledge Economy), Korea, under the ITRC (Information Technology Research Center) support program supervised by the IITA (Institute of Information Technology Assessment).

S. Erküçük was with the School of Engineering Science, Simon Fraser University, Burnaby, BC V5A 1S6, Canada. He is now with the Department of Electronics Engineering, Kadir Has University, Cibali, 34083, Istanbul, Turkey (e-mail: serkucuk@khas.edu.tr).

D. I. Kim is with the School of Information and Communication Engineering, Sungkyunkwan University, Suwon 440-746, Korea (e-mail: dikim@ece.skku.ac.kr).

K. S. Kwak is with the UWB-ITRC, Inha University, Incheon, 402-751 Korea (e-mail: kskwak@inha.ac.kr).

Digital Object Identifier 10.1109/TWC.2008.070314.

II. System Models

An analogy can be made between MCSK and MPPM as they both use one of the M pulse locations to transmit information. Therefore, the signalling structures should be clearly defined for a fair comparison. Let us initially start with TH-MPPM. The signal that is used to transmit the ith symbol of the kth user using conventional TH-MPPM can be modelled as

$$s_{MPPM}^{(k)}(t) = \sqrt{\frac{E_s}{N_s}} \sum_{j=(i-1)N_s}^{iN_s-1} w\Big(t - jT_f - c_{j'}^{(k)} T_c - d_i{}^{(k)} \delta_d\Big) \quad (1)$$

where $w(t)$ denotes the transmitted pulse, which includes the effects of transmitting and receiving antennas, with unit energy and pulse width T_p, T_f is the frame time (in average, one pulse is transmitted every frame time), N_s is the number of pulses used to transmit one symbol, $T_s = N_s T_f$ is the symbol duration, and E_s is the symbol energy. $\mathbf{c}^{(k)} = [c_0^{(k)}\ c_1^{(k)}\ \cdots\ c_{N_p-1}^{(k)}]^T$ is the kth user's N_p-long TH code consisting of integers, where $N_p \geq N_s$ and $j' = (j \mod N_p)$. For reduced collisions, it is assumed that $c_{j'}^{(k)}$ is uniformly distributed over $[0, N_h - 1]$. To prevent inter-symbol interference (ISI), $N_h T_c + M\delta_d + T_m \leq T_f$, where $T_c \geq T_p$ is the chip time, δ_d is the time shift parameter of MPPM and T_m is the maximum delay spread. $d_i{}^{(k)} \in \{0, \ldots, M-1\}$ carries the ith symbol information of the kth user and $\delta_d = T_c$ is selected to allow for orthogonal pulse locations. Using MPPM,

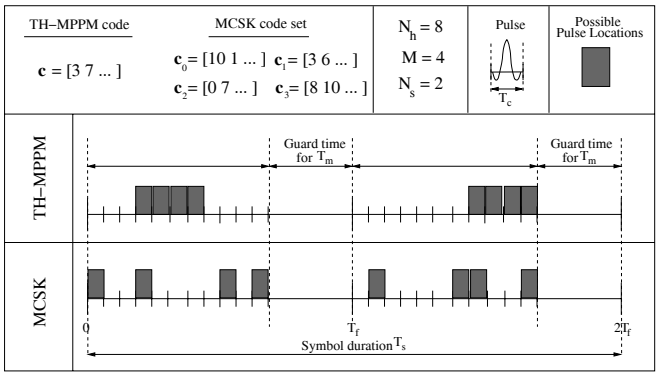

Fig. 1. Illustration for TH-MPPM and MCSK transmit structures.

a pulse is initially shifted to one of the N_h TH locations, and further shifted to one of the M *consecutive* data-bearing pulse locations within a frame time T_f.

As opposed to consecutive fixed pulse positions in MPPM, MCSK transmits pulses at randomized locations determined by M TH codes. Accordingly, MCSK combines the TH shift and the PPM shift in (1) and achieves data transmission through one of the M TH codes as

$$s^{(k)}_{MCSK}(t) = \sqrt{\frac{E_s}{N_s}} \sum_{j=(i-1)N_s}^{iN_s-1} w\Big(t - jT_f - c^{(k)}_{d_i^{(k)},\,j'} T_c\Big) \quad (2)$$

where $\left\{0 \le c^{(k)}_{d_i^{(k)},\,j'} < N_h + M - 1; \forall j', \forall k\right\}$ is equivalent to the combined TH and PPM shift effect in MPPM and $d_i^{(k)} \in \{0, \ldots, M-1\}$ selects one of the M TH codes of user k. Contrary to a single TH code $\mathbf{c}^{(k)}$ being assigned to each user in TH-MPPM, a TH code set consisting of M TH codes $\mathbf{C}^{(k)} = [\mathbf{c}_0^{(k)}\, \mathbf{c}_1^{(k)} \cdots \mathbf{c}_{M-1}^{(k)}]$ is assigned to each user in MCSK, where $\mathbf{c}_m^{(k)} = [c_{m,0}^{(k)} \cdots c_{m,N_p-1}^{(k)}]^T$. Each TH code set is generated independently for each user to allow for multiple access. In each TH code set, the codes are designed to satisfy $\{c^{(k)}_{0,j'} \neq \ldots \neq c^{(k)}_{M-1,j'}, \forall j', \forall k\}$ to ensure orthogonal locations for the transmit pulse. For reduced collisions, it is further assumed that $c^{(k)}_{m,j'}$ is uniformly distributed over $[0, N_h + M - 2]$ while conforming to the TH code design constraints above. With these TH code sets, MCSK randomizes locations of the transmit pulse within each frame time. For better understanding of the differences between TH-MPPM and MCSK, their signalling structures are illustrated in Fig. 1 for a single-user when $N_h = 8$, $M = 4$, $N_s = 2$ for the given TH codes.

For a multiple-access system consisting of N_u users with perfect power control, the received signal $r(t)$ at the output of the receive antenna can be modelled as

$$r(t) = \sum_{k=1}^{N_u} s^{(k)}(t - \tilde{\tau}_k) \otimes h_k(t) + n(t) \quad (3)$$

where $h_k(t)$ is the kth user's channel impulse response (CIR), $\otimes$ is the convolution operator, $\tilde{\tau}_k$ is the time asynchronism between the users and $n(t)$ is the additive white Gaussian noise (AWGN) with two-sided power spectral density $N_0/2$. $h_k(t)$ is given as [5]

$$h_k(t) = \sum_{l=0}^{L-1} h_{k,l}\delta(t - \tau_{k,l}) \quad (4)$$

with the normalization assumption $\sum_{l=0}^{L-1} h_{k,l}^2 = 1$, $\forall k$ that removes the path loss factor, where $h_{k,l}$ is the kth channel's lth multipath coefficient, $\tau_{k,l}$ is the delay of the kth channel's lth multipath component and $\delta(\cdot)$ is the Dirac delta function. For the accurate τ-spaced channel model, $\{\tau_{k,l}\}$ and $\{h_{k,l}\}$ take the exact values for the given CIR, whereas for the commonly used approximate T_c-spaced channel model, $\{\tau_{k,l}\}$'s are quantized to the nearest integer multiple of T_c (i.e., $l \cdot T_c$) with the corresponding $\{h_{k,l}\}$ summed up and normalized accordingly [6].

Assuming a partial-Rake receiver with L_p fingers, perfectly estimated CIR coefficients for user 1 and T_c-spaced channel model for simplicity in analysis, the correlator output statistics of the first user $\{D_m^{(1)}\}$ for the first symbol transmitted in a multipath channel are computed as

$$D_m^{(1)} = \sqrt{\frac{N_s}{E_s}} \sum_{j=0}^{N_s-1} \sum_{l=0}^{L_p-1} h_{1,l} \int_{jT_f}^{(j+1)T_f} r(t)\, w^{(1)}_{m,temp}(t)\, dt \quad (5)$$

for $\{m = 0, \ldots, M-1\}$, where $w^{(1)}_{m,temp}(t) = w\Big(t - jT_f - c^{(1)}_{m,j}T_c - lT_c\Big)$ is the template waveform used by MCSK. For MPPM, $c^{(1)}_{m,j}$ should be replaced by $(c_j^{(1)} + m)$ in the template waveform. Given that $d_0^{(1)}$ is transmitted,[1] (5) can be simplified for both MCSK and MPPM as

$$D_m^{(1)} = S_m + I_m + N_m \quad (6)$$

where S_m is the output signal term, I_m is the MUI term and N_m is the output noise term. S_m and N_m can be given for MCSK as

$$\begin{aligned} S_m &= \sum_{j=0}^{N_s-1} \sum_{l=0}^{L_p-1} h_{1,l} h_{1,(l+c_{m,j}-c_{d_0,j})} \\ N_m &= \sum_{j=0}^{N_s-1} \sum_{l=0}^{L_p-1} h_{1,l} n_{(j,l+c_{m,j}-c_{d_0,j})} \end{aligned} \quad (7)$$

where $h_{1,l} = 0$ for $l < 0$, and $\left\{n_{(a,b)}; \forall a, \forall b\right\}$ are independent noise random variables with $\sigma_n^2 = \frac{N_s}{2E_s/N_0}$. For MPPM, $(c_{m,j} - c_{d_0,j})$ should be replaced by $(m - d_0)$ for the calculation of S_m and N_m. The common interference term I_m for MCSK and MPPM is

$$\begin{aligned} I_m = \sqrt{\frac{N_s}{E_s}} \sum_{j=0}^{N_s-1} \sum_{l=0}^{L_p-1} \sum_{k=2}^{N_u} h_{1,l} \\ \times \int_{jT_f}^{(j+1)T_f} \Big(s^{(k)}(t - \tilde{\tau}_k) \otimes h_k(t)\Big) w^{(1)}_{m,temp}(t)\, dt. \end{aligned} \quad (8)$$

The transmitted symbol d_0 is then estimated as

$$\mathbf{argmax}\left\{D_m^{(1)}\right\} \;\Rightarrow\; m \;\Rightarrow\; \hat{d}_0. \quad (9)$$

[1]The user index (1) of $d_0^{(1)}$ and $\mathbf{c}_m^{(1)}$ is omitted in the following text for notational convenience.

III. Analysis of the Symbol-Error Rate

The transmitted symbol d_0 will be detected correctly at the receiver if $D_{d_0}^{(1)} > D_m^{(1)}$, $\forall m, m \neq d_0$. Accordingly, the probability of error given that d_0 is transmitted, can be formulated as

$$P(e|d_0) = \Pr\Big[\bigcup_{\substack{m=0 \\ m\neq d_0}}^{M-1} S_{d_0,m} + I_{d_0,m} + N_{d_0,m} < 0 \,\Big|\, d_0\Big], \quad (10)$$

where $S_{d_0,m} = (S_{d_0} - S_m)$, $I_{d_0,m} = (I_{d_0} - I_m)$, and $N_{d_0,m} = (N_{d_0} - N_m)$. For convenience, we here define $P_e(m|d_0)$, the *pair-wise* error probability of receiving m, given that d_0 is transmitted, as

$$P_e(m|d_0) = \Pr\Big[S_{d_0,m} + I_{d_0,m} + N_{d_0,m} < 0 \,\Big|\, d_0\Big]. \quad (11)$$

Since the $M-1$ pair-wise error probabilities $\{P_e(m|d_0)\}$ are mutually dependent, an exact SER expression, P_e, is difficult to obtain. Hence, the upper bound on P_e can be obtained as

$$\sum_{d_0=0}^{M-1} \sum_{\substack{m=0 \\ m\neq d_0}}^{M-1} P_e(m|d_0) P(d_0) \geq P_e \quad (12)$$

where $P(d_0)$ is the probability of d_0 being transmitted.

A. Single-user case

In MCSK, each distinct (d_0, m)-pair refers to the selection of independent TH codes. Therefore, $P_{e,MCSK}(m|d_0)$ is a function of $\big(c_{d_0,j} - c_{m,j}\big)$, where $\big\{c_{m,j},\, \forall m, \forall j\big\}$ are assumed to be uniformly distributed over $[0, N_h + M - 2]$ with the condition $c_{d_0,j} \neq c_{m,j}$. Hence, the difference $C_j = \big(c_{d_0,j} - c_{m,j}\big)$ has the probability density function (pdf)

$$f_{C_j}(x) = \sum_{\substack{C_j=-(N_h+M-2) \\ C_j\neq 0}}^{N_h+M-2} \frac{(N_h+M-1) - |C_j|}{(N_h+M-1)(N_h+M-2)}\, \delta\big(x - C_j\big) \quad (13)$$

when considered for every j value. Since C_j is independent $\forall j, j \in [0, N_s - 1]$, $S_{d_0,m}$ and $N_{d_0,m}$ become functions of $\big\{C_j | j = 0, \ldots, N_s - 1\big\}$, which indicates the combinations of different C_j values. Accordingly, the instantaneous error probability $P_{e,MCSK}(m|d_0)$ (i.e., for one channel realization) can be derived as

$$\begin{aligned} P_{e,MCSK}(m|d_0) = & \sum_{\substack{C_0=-(N_h+M-2) \\ C_0\neq 0}}^{N_h+M-2} \frac{(N_h+M-1) - |C_0|}{(N_h+M-1)(N_h+M-2)} \\ & \cdots \sum_{\substack{C_{N_s-1}=-(N_h+M-2) \\ C_{N_s-1}\neq 0}}^{N_h+M-2} \frac{(N_h+M-1) - |C_{N_s-1}|}{(N_h+M-1)(N_h+M-2)} \\ & \times Q\left(\sqrt{SNR_{d_0,m}\big(\{C_j\}\big)}\right) \end{aligned} \quad (14)$$

where $Q(\cdot)$ is the Q-function and $SNR_{d_0,m}\big(\{C_j\}\big)$ is the output signal-to-noise ratio (SNR) of the decision variable. Assuming the channel coefficients $\{h_{1,l}\}$ are known and a partial-Rake receiver with L_p fingers are used, $SNR_{d_0,m}\big(\{C_j\}\big)$ can be computed using (7) and is given by

$$\begin{aligned} SNR_{d_0,m}\big(\{C_j\}\big) &= \frac{|S_{d_0,m}\big(\{C_j\}\big)|^2}{\sigma^2_{N_{d_0,m}(\{C_j\})}} \\ &= \frac{2E_s}{N_0} H\big(\{C_j\}, L_p\big) \end{aligned} \quad (15)$$

where $H\big(\{C_j\}, L_p\big) = \frac{\Big[\sum_{j=0}^{N_s-1} \sum_{l=0}^{L_p-1} \big(h_{1,l}^2 - h_{1,l} h_{1,(l-C_j)}\big)\Big]^2}{N_s \sum_{j=0}^{N_s-1} \sum_{l'_1,l'_2,l'_3} \big(h_{1,l'} - h_{1,(l'+C_j)}\big)^2}$.

Here, the summation regions l'_1, l'_2 and l'_3 are defined as $\{l'_1 | -C_j \leq l' \leq -1\}$, $\{l'_2 | 0 \leq l' \leq L_p - 1\}$ and $\{l'_3 | L_p \leq l' \leq L_p - 1 - C_j\}$, where these regions may or may not exist depending on the value of C_j. Also, it should be noted that $h_{1,l} = 0$ for only $l < 0$, whereas $h_{1,l'} = 0$ for $l' < 0$ and $l' > L_p - 1$.

For TH-MPPM, $C_j = \big(c_{d_0,j} - c_{m,j}\big)$ should be replaced by $(d_0 - m)$, which has a fixed value for a given (d_0, m)-pair. Accordingly, (14) takes the form $P_{e,MPPM}(m|d_0) = Q\big(\sqrt{SNR_{d_0,m}}\big)$ where $SNR_{d_0,m} = \frac{2E_s}{N_0} \cdot H(d_0, m, L_p)$, and $H(d_0, m, L_p) = \frac{\Big[\sum_{l=0}^{L_p-1} \big(h_{1,l}^2 - h_{1,l} h_{1,(l-(d_0-m))}\big)\Big]^2}{\sum_{l'_1,l'_2,l'_3} \big(h_{1,l'} - h_{1,(l'+(d_0-m))}\big)^2}$ with the similar summation regions given after (15) if C_j is replaced by $(d_0 - m)$.

By comparing $H\big(\{C_j\}, L_p\big)$ with $H(d_0, m, L_p)$, two apparent advantages of MCSK over MPPM can be observed. First of all, the interference terms $\{h_{1,(l-C_j)}\}$ in MCSK are more distant from the desired terms $\{h_{1,l}\}$ compared to the interference terms $\{h_{1,(l-(d_0-m))}\}$ in MPPM, since C_j can take larger values compared to $(d_0 - m)$. Accordingly, for a decaying power delay profile, it is expected that the interference caused by multipath-delayed pulses will have less effect on the decision variables of MCSK. Secondly, $\{C_j\}$ are independent for $\{j = 0, \ldots, N_s - 1\}$. Therefore, combining independent $\{C_j\}$ increases the *time diversity* and it is expected that the performance gain of MCSK over MPPM will increase with N_s increasing, since MPPM is independent of N_s for the single-user case.

B. Multi-user case

One approach for the accurate modelling of MUI distributions is the *generalized* Gaussian distributions (GGDs) used in [4]. For an accurate *semi-analytic* SER expression, each channel realization should have its own GGD for modelling the MUI, which makes the SER evaluation computationally complex. With the motivation of providing a computationally efficient and yet an accurate SER evaluation, some approximations are considered for GGDs in the Results Section when modelling the MUI distribution.

Modelling the MUI term with the GGD is a two-step procedure as proposed in [4]. For an accurate SER expression, MUI distributions should be obtained *individually* for each channel realization of user 1. For that, $I_{d_0,m} = (I_{d_0} - I_m)$ is simulated using (8) for the given channel realization $\{h_{1,l}\}$ with various channel realizations $\{h_k(t)\}$ and time asynchronism values $\{\tilde{\tau}_k\}$ of $N_u - 1$ interfering users for $\{C_j\}$-values or for each (d_0, m)-pair depending on the modulation. The distribution of $I_{d_0,m}$ is then fitted into the GGD resulting in $f_{I_{d_0,m}}(x)$. The details of the modelling of $f_{I_{d_0,m}}(x)$ can be obtained from

[4]. Once $f_{I_{d_0,m}}(x)$ is determined, the characteristic function (CF) method can be used to evaluate the error probability as in [7]. By calculating[2] the CF's of $I_{d_0,m}$ and $N_{d_0,m}$, and the deterministic value of $S_{d_0,m}$ for each channel realization, $P_e(m|d_0)$ can be accurately evaluated.

For the error probability evaluation of MCSK for each channel realization, let us rewrite $P_e(m|d_0)$ given in (11) as $P_e(m|d_0) = \Pr\left[S_{d_0,m} + \Lambda_{d_0,m} < 0 \,\middle|\, d_0\right]$ where $\Lambda_{d_0,m} = I_{d_0,m} + N_{d_0,m}$. Due to the independence of the MUI and noise terms, the CF of $\Lambda_{d_0,m}$ can be expressed as $\Phi_{\Lambda_{d_0,m}}(\omega) = \Phi_{I_{d_0,m}}(\omega) \cdot \Phi_{N_{d_0,m}}(\omega)$, where the CF's of the MUI and noise terms are

$$\Phi_{I_{d_0,m}}(\omega) = \int_{-\infty}^{\infty} e^{j\omega x} f_{I_{d_0,m}}(x)\, dx = \sum_{n=0}^{\infty} \frac{(j\omega)^n}{n!} \mu_n \quad (16)$$

$$\Phi_{N_{d_0,m}}(\omega) = \int_{-\infty}^{\infty} e^{j\omega x} f_{N_{d_0,m}}(x)\, dx = e^{-\sigma^2_{N_{d_0,m}} \omega^2/2} \quad (17)$$

with $\sigma^2_{N_{d_0,m}} = \frac{N_s}{2E_s/N_0} \sum_{j=0}^{N_s-1} \sum_{l'_1,l'_2,l'_3} \left(h_{1,l'} - h_{1,(l'+C_j)}\right)^2$ for MCSK. For TH-MPPM, C_j in $\sigma^2_{N_{d_0,m}}$ should be replaced by $(d_0 - m)$. In (16), μ_n is the nth-order moment of the GGD [8], where odd-order moments are zero due to the symmetrical distribution of a GGD around zero, and even-order moments can be numerically calculated from [4, eq. (13)]. After taking the inverse transform of $\Phi_{\Lambda_{d_0,m}}(\omega)$ as in [7], the cumulative distribution function of $\Lambda_{d_0,m}$ can be expressed as

$$F_{\Lambda_{d_0,m}}(x) = \frac{1}{2} + \frac{1}{\pi} \int_0^{\infty} \frac{\sin(x\omega)}{\omega} \Phi_{\Lambda_{d_0,m}}(\omega)\, d\omega. \quad (18)$$

For MCSK, $P_e(m|d_0)$ depends on the pdf of C_j given in (13) for each (d_0, m)-pair. Accordingly, the instantaneous error probability $P_e(m|d_0)$ of MCSK can be evaluated as

$$\begin{aligned} P_{e,MCSK}(m|d_0) &= \Pr\left[S_{d_0,m}(\{C_j\}) + \Lambda_{d_0,m}(\{C_j\}) < 0 \,\middle|\, d_0\right] \\ &= \sum_{\substack{C_0 \neq 0 \\ C_0 = -(N_h+M-2)}}^{N_h+M-2} \frac{(N_h+M-1) - |C_0|}{(N_h+M-1)(N_h+M-2)} \\ &\quad \cdots \sum_{\substack{C_{N_s-1} \neq 0 \\ C_{N_s-1} = -(N_h+M-2)}}^{N_h+M-2} \frac{(N_h+M-1) - |C_{N_s-1}|}{(N_h+M-1)(N_h+M-2)} \\ &\quad \times \left[1 - F_{\Lambda_{d_0,m}(\{C_j\})}\left(S_{d_0,m}(\{C_j\})\right)\right] \quad (19) \end{aligned}$$

where $S_{d_0,m}(\{C_j\})$ and $F_{\Lambda_{d_0,m}(\{C_j\})}$ can be obtained from (7), (16) – (18). For TH-MPPM, $P_e(m|d_0)$ depends on the unique (d_0, m)-pair and can be evaluated as $P_{e,MPPM}(m|d_0) = 1 - F_{\Lambda_{d_0,m}}(S_{d_0,m})$. It should be noted that the multi-user case SER expression given in (19) becomes equal to the single-user case expression given in (14) when $\Phi_{I_{d_0,m}}(\omega)$ in (16) is unity.

IV. Results

In this section, the SER bounds for MCSK and TH-MPPM are validated in the approximate T_c-spaced channel model for both single- and multi-user cases. In all the analysis and simulations, the commonly considered Gaussian monocycle of [1] with pulse width $T_p = 0.6$ ns and chip time $T_c = 0.6$ ns are used. For $T_p = 0.6$ ns, the T_c-spaced channel model does not consider possible pulse overlappings [6]. Therefore, simulation studies are also conducted in the accurate τ-spaced channel, which takes into account the inter-pulse interferences. In any case, the SER expressions derived in the commonly used T_c-spaced channel model are accurate for shorter duration pulses (e.g., 0.1 ns). The TH code period N_p is assumed to be infinity without loss of generality. The frame times are selected as $T_f = 60$ ns and $T_f = 120$ ns for the IEEE 802.15.3a CM1 and CM3 channel types [9], respectively, in order to prevent ISI. While shorter T_f would provide increased data rate at the expense of degraded performance due to ISI, the selected T_f values eliminate the ISI components, making self-user interference, MUI and AWGN the only sources of interferences.

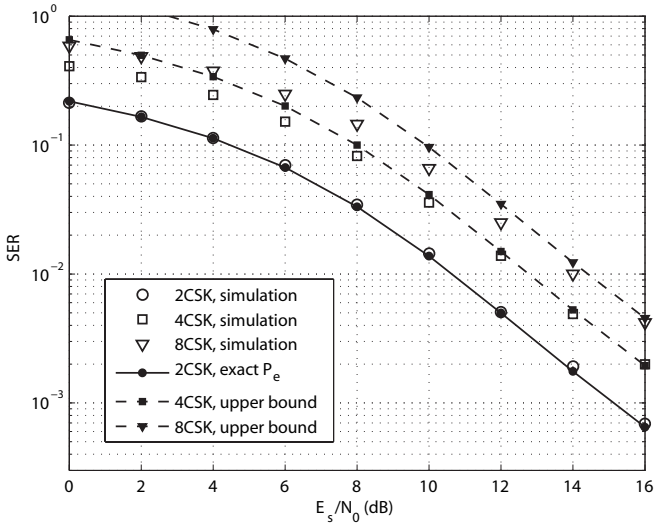

Fig. 2. Bounds on the SER of MCSK when $N_s = 2$.

A. Performances for the single-user case

In order to validate the analysis, the SER bound given in (12) is evaluated for MCSK and TH-MPPM in CM1 by averaging over 10^3 channel realizations, and verified by simulations for different N_s values ($N_s = \{1, 2, 4\}$) when $L_p = 8$ Rake fingers are used. Maximum shift of MCSK is fixed to $(N_h + M - 2) = 31$ for different M values, which control the value of N_h.

For 2CSK and 2PPM, the upper bound becomes the error probability P_e due to $P_e(m|d_0)$ taking a single value for every d_0. For $\{4\text{CSK}, 8\text{CSK}\}$ and $\{4\text{PPM}, 8\text{PPM}\}$, the simulated performances approach the upper bound for medium and high SNR values. Accordingly, the derived upper bound can be used to approximate the SER performances in the medium and high SNR regions. In Fig. 2, the SER bounds of MCSK are plotted for $N_s = 2$. When the SER range $[10^{-2}, 10^{-3}]$ is considered, MCSK can provide 1-2 dB performance gain over MPPM. This net performance gain will be discussed in the next paragraph.

Next, the accurate τ-spaced channel model is considered to

[2]For MCSK, the terms $S_{d_0,m}$, $I_{d_0,m}$ and $N_{d_0,m}$ are functions of $\{C_j\}$. Accordingly, these terms should be associated with $\{C_j\}$ whenever MCSK is considered.

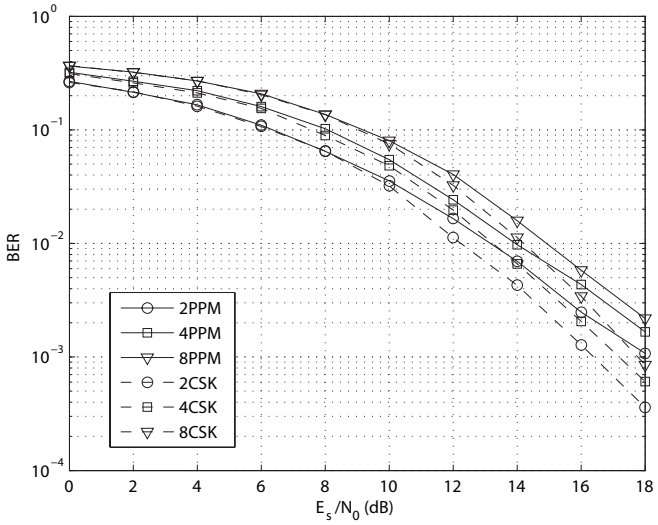

Fig. 3. Performances of TH-MPPM and MCSK for practical implementation of a partial-Rake receiver with $L_p = 10$ fingers in the accurate τ-spaced channel for CM1.

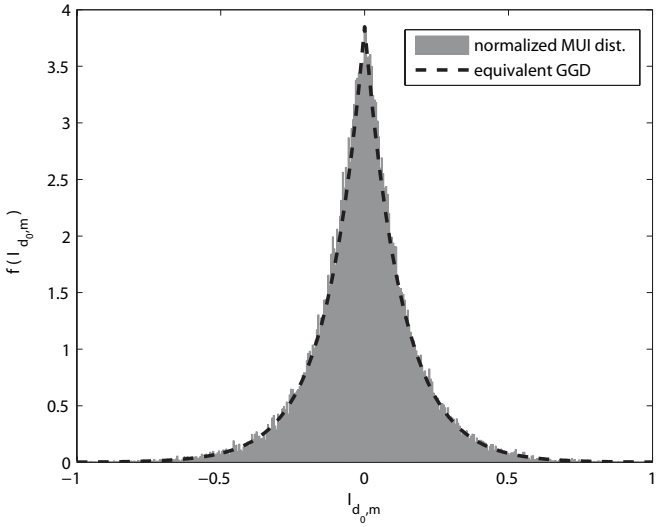

Fig. 4. The MUI distribution obtained by simulations and its equivalent generalized Gaussian distribution.

provide more realistic performance results. In the simulation studies, it is assumed that the channel coefficients are perfectly estimated and the locations of the Rake fingers are determined by the search algorithm presented in [6]. In Fig. 3, bit-error rate (BER) performances of MCSK and TH-MPPM are compared in CM1 when a partial-Rake ($L_p = 10$) receiver is considered for $N_s = 2$. It can be observed that MCSK can provide about 1.5-2 dB performance gain over MPPM at BER $= 2 \cdot 10^{-3}$. When $N_s = 1$, while MPPM performs the same, it is observed that the performance gain of MCSK is decreased to 1-1.5 dB. Accordingly, this performance gain is a result of *only* the randomizing effect, whereas the performance gain for $N_s > 1$ is determined by time diversity as well as the randomizing effect. When $N_s = 4$, MCSK provides additionally 0.2-0.3 dB performance gain with respect to the $N_s = 2$ case. While increasing N_s slightly improves the performance beyond the case of $N_s = 2$, it linearly reduces the data rate. Accordingly, $N_s = 2$ is a reasonable selection for the single-user case as it provides high data rate and yet can achieve time diversity.

Besides the line-of-sight (LOS) CM1 channel type, system performances are compared in the non-LOS (NLOS) CM3 channel type. For the maximum TH shift considered for MCSK ($\approx$ 19 ns) in this study, CIR coefficients in CM1 become very small at the maximum shift.[3] When a CM3 channel type is considered, the CIR coefficients are still significant even at the maximum shift. Accordingly, the system performance of MCSK is not expected to benefit from pulse location randomization. However, time diversity achieved by combining different pulse locations for $N_s > 1$ may increase the performance. In the simulation studies conducted, MCSK and TH-MPPM performed almost the same for $N_s = 1$, whereas MCSK provided about 0.2-0.5 dB performance gain at BER $= 10^{-2}$ for $N_s = 2$, which confirm the above explanations.

B. Performances for the multi-user case

For the multi-user case analysis, 2PPM is considered as a special case of 2CSK, where the SER bounds for {4PPM, 8PPM} can be found similarly. SER of MCSK can also be evaluated similarly by considering various C_j values for a given N_h. Here, some assumptions and approximations are given to yield the analysis computationally efficient.

For the *exact* evaluation of $P_{e,MPPM}(m|d_0)$, initially the GGD of the MUI, $f_{I_{d_0,m}}(x)$, should be obtained for each channel realization and (d_0, m)-pair. Each channel realization should have its own GGD since the values of $S_{d_0,m}$ and $N_{d_0,m}$ change with channel realizations. However, this requires many simulations. Therefore, it is assumed that a *single* MUI distribution is obtained by simulating (8) over various channel realizations for the first-order approximation. In Fig. 4, the MUI distribution of $N_u - 1 = 7$ interfering users obtained over 10^3 channel realizations[4] of user 1 and its equivalent GGD $f_{I_{d_0,m}}(x)$ are plotted for $(d_0 = 0, m = 1)$. Using the single distribution of $f_{I_{d_0,m}}(x)$ in (16) and the 10^3 channel realizations of user 1 in $S_{d_0,m}$ and in (17), 10^3 instantaneous values of (18) are obtained to calculate the average SER of $P_{e,MPPM}(m|d_0)$.

In Fig. 5, numerical values for SER are compared to the simulation values for partial-Rake and all-Rake receivers labelled with (P) and (A), respectively. Here, analysis-1 refers to the calculation of $P_{e,MPPM}(m|d_0)$ using the first-order approximation that considers only a single GGD, which is different for partial-Rake and all-Rake. It can be observed that the numerical values for analysis-1 deviate from the simulation values for the medium and high SNR regions.

[3]If the pulses were *continuously* transmitted at maximum separated locations, although the system performance could have improved, the PSD would have spectral components due to limited TH randomization that would violate the FCC spectral mask [10]. MCSK that transmits at randomized pulse locations eliminates this problem.

[4]The number 10^3 is selected arbitrarily. 10^3 channel realizations can yet successfully represent a GGD. With this selection, numerical analysis is computationally more efficient than simulation studies as will be discussed at the end of the section.

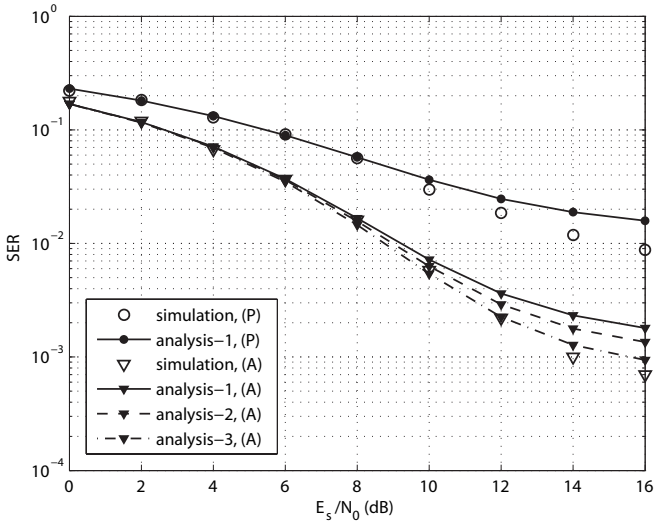

Fig. 5. SER evaluation in the presence of $N_u - 1 = 7$ interfering users that are modelled by GGD.

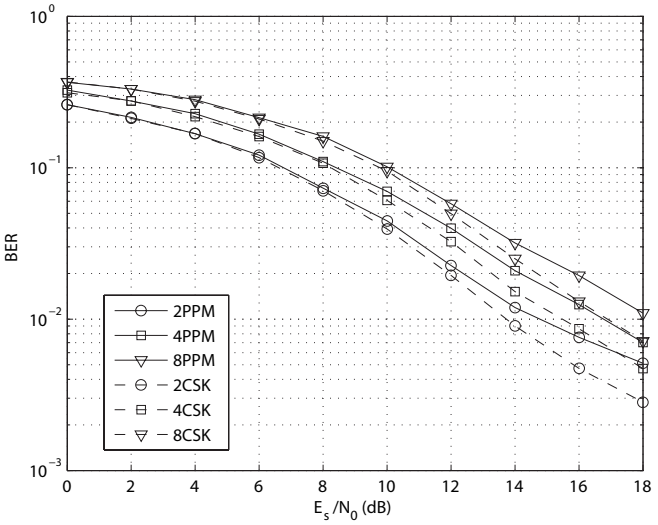

Fig. 6. Performances of TH-MPPM and MCSK for practical implementation of a partial-Rake receiver with $L_p = 10$ fingers in the accurate τ-spaced channel for CM1 when $N_u = 8$ users are present.

By increasing the number of GGDs in the evaluation of $P_{e,MPPM}(m|d_0)$, more accurate results can be obtained. Considering the range of $S_{d_0,m}$ values[5] obtained from (7), more GGDs are considered for the error probability evaluation as the second-order approximation. For analysis-2 (using 2 GGDs) and analysis-3 (using 4 GGDs), channel realizations that result in $S_{d_0,m} \approx \{0.8, 1.2\}$ and $S_{d_0,m} \approx \{0.4, 0.8, 1.2, 1.6\}$ are used in determining the independent MUI distributions, respectively. For the evaluation of $P_{e,MPPM}(m|d_0)$, initially the 10^3 channel realizations of user 1 are used in $S_{d_0,m}$. Each obtained $S_{d_0,m}$ value is then rounded to the nearest value above to select the corresponding GGD to be used in each channel realization. Then, using the selected GGD of $f_{I_{d_0,m}}(x)$, the average SER of $P_{e,MPPM}(m|d_0)$ is calculated similar to the first-order approximation. In Fig. 5, it can be observed that the SER performance approximation becomes better with increasing number of GGDs. Even with four GGDs representing the MUI distribution, the semi-analytic SER expression values converge to the simulation values.

The numerical analysis of the multi-user case is computationally more efficient than the simulation study. In the simulation study, approximately 10^5 simulations should be run to achieve convergence for 10^{-3} BER for each SNR value. In the numerical analysis, 10^3 simulation runs are conducted for each GGD, where each GGD can use the closed-form expression in (16) to obtain the CF of the MUI term. Considering that only a few GGDs are adequate for the analysis and (18) can be evaluated numerically, the computation time of the analysis is much shorter than that of the simulation study. Moreover, once a GGD is obtained, it is used for all the SNR values, as opposed to repeating the sets of channel realizations in the simulation for each SNR value.

Next, the accurate τ-spaced channel model is considered to provide more realistic performance results. In Fig. 6, BER performances of MCSK and TH-MPPM are compared in CM1 for a partial-Rake ($L_p = 10$) receiver when $N_s = 2$ and $N_u = 8$. It can be observed that MCSK can provide about 1.5-2 dB performance gain over MPPM for the BER range $[10^{-2}, 5 \cdot 10^{-3}]$. Similar to the observations made for the single-user case, only the randomizing effect determines the performance gain when $N_s = 1$, whereas the time diversity is also effective when $N_s > 1$.

Finally, some comments are provided on the complexity of MCSK compared to TH-MPPM. While the data rates and number of supported users are the same for both modulations, the increased performance gain of MCSK is mainly a result of increased number of TH codes.[6] The increased number of TH codes may modestly increase the signal processing when selecting pulse locations at the transmitter and receiver. However, the number of correlations for the given template waveform and the Rake processing in each frame will be the same for both modulations.

V. Conclusion

In this paper, MCSK impulse modulation was studied in detail to quantify its performance improvement over the conventional TH-MPPM. For the single-user case, the effect of multipath-delayed pulses on M decision variables was explicitly provided in terms of channel impulse response coefficients. For the multi-user case, an accurate semi-analytic SER expression was derived based on modelling the MUI terms with the GGD. Some approximations to MUI modelling were made that increased the computational efficiency of numerical analysis. The study showed that MCSK can provide about 2 dB performance gain over MPPM as it reduces the effects of multipath delays on the decision variables by randomizing locations of the transmit pulse.

[5]For 10^3 channel realizations considered, $S_{d_0,m}$ values were in the range [0.4,1.6].

[6]A set of M distinct TH codes for MCSK can be shared among users, where additional user-specific TH codes can be used to differentiate users. In this case, the total number of TH codes for an N_u-user MCSK system is $(N_u + M)$.

REFERENCES

[1] M. Z. Win and R. A. Scholtz, "Ultra-wide bandwidth time-hopping spread-spectrum impulse radio for wireless multiple-access communications," *IEEE Trans. Commun.*, vol. 48, pp. 679–691, Apr. 2000.

[2] F. Ramirez-Mireles, "Performance of ultrawideband SSMA using time hopping and M-ary PPM," *IEEE J. Select. Areas Commun.*, vol. 19, pp. 1186–1196, June 2001.

[3] S. Erküçük and D. I. Kim, "M-ary code shift keying impulse modulation combined with BPPM for ultra wideband communications," *IEEE Trans. Wireless Commun.*, vol. 6, pp. 2255–2265, June 2007.

[4] J. Fiorina, "A simple IR-UWB receiver adapted to multi-user interferences," in *IEEE Proc. GLOBECOM '06*, Nov. 2006.

[5] A. Molisch, "Ultrawideband propagation channels-theory, measurement, and modeling," *IEEE Trans. Veh. Technol.*, vol. 54, pp. 1528–1545, Sept. 2005.

[6] S. Erküçük, D. I. Kim, and K. S. Kwak, "Effects of channel models and Rake receiving process on UWB-IR system performance," in *IEEE Proc. ICC '07*, June 2007.

[7] B. Hu and N. C. Beaulieu, "Accurate evaluation of multiple-access performance in TH-PPM and TH-BPSK UWB systems," *IEEE Trans. Commun.*, vol. 52, pp. 1758–1766, Oct. 2004.

[8] M. Abramowitz and I. A. Stegun, *Handbook of Mathematical Functions with Formulas, Graphs, and Mathematical Tables*. New York: Dover, 1972.

[9] J. R. Foerster *et. al.* , "Channel Modeling Subcommittee Final Report," Doc. IEEE P802.15-02/490r1, SG3a, Feb. 2003.

[10] S. Erküçük and D. I. Kim, "Spectral characteristics of M-ary code shift keying based impulse radios: effects of code design," *IEEE Trans. Wireless Commun.*, vol. 6, pp. 2266–2275, June 2007.